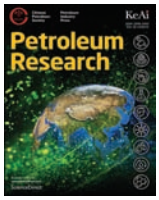
Petroleum Research 11 (2026) 789–798

Contents lists available at ScienceDirect

Petroleum Research

journal homepage: http://www.keaipublishing.com/en/journals/petroleum-research/



Full Length Article

Preparation and mechanistic analysis of high-selectivity water control systems



Zhizhen Li [a,*], Weiyu Chen [a,b,c], Yanhui Su [a,b,c], Xueli Geng [a], Bin Shi [a], Xiaobin Zheng [a], Qian Zhou [d], Gang Xie [d]

[a] CNOOC EnerTech-Drilling & Production Co., Tanggu, Tianjin, 300452, China
[b] State Key Laboratory of Offshore Oil and Gas Exploition, Beijing, 100028, China
[c] CNOOC Energy Technology & Services Limited Key Laboratory of Enhanced Oil Recovery, Tanggu, Tianjin, 300452, China
[d] State Key Laboratory of Oil & Gas Reservoir Geology and Exploitation, Southwest Petroleum University, Chengdu, Sichuan, 610500, China

ARTICLE INFO

Article history:
Received 27 March 2025
Received in revised form
22 November 2025
Accepted 23 November 2025
Available online 28 November 2025

Keywords:
High-selectivity
Oil solubility
Water control
Oil-in-water emulsion

ABSTRACT

This paper presents a highly selective water control system designed to address declining oil production in offshore wells caused by rising water cuts while overcoming the poor selectivity of current chemical water control materials. The system was developed by copolymerizing octadecyl methacrylate and butyl methacrylate, followed by emulsion polymerization to prepare oil-soluble polymers. This resulted in a water-dispersible, high-selectivity water control system in the form of an emulsion dispersion. The feasibility of its field application was assessed via median particle size and reservoir stability tests, and the system's water control performance, visual performance, and underlying mechanism were evaluated. The test results showed that the median droplet diameter of the emulsion in the system was 0.431 μm, and it remained stable for at least 8 h under reservoir conditions. The system demonstrated excellent selective water-control capabilities, with a water-phase permeability blocking rate of 82.42% and an oil-phase permeability blocking rate of 5.02%. The mechanism of action was further explored via visualized flat plate tests and low-field nuclear magnetic resonance scanning displacement experiments on rock cores. The findings suggest that oil-soluble particles exhibit effective selective water-control performance and can be applied in water control operations in offshore oil fields.

© 2025 Chinese Petroleum Society. Publishing services by Elsevier B.V. on behalf of KeAi Communications Co. Ltd. This is an open access article under the CC BY-NC-ND license (http://creativecommons.org/licenses/by-nc-nd/4.0/).

1. Introduction

The development and utilization of energy resources are critical determinants of economic growth and sustainable development (Yonguep et al., 2022). In petroleum engineering, waterflooding is the most widely employed and economically favorable enhanced oil recovery technique; it is primarily used to maintain reservoir pressure and efficiently drive crude oil into production wells (Anikin et al., 2025; Li et al., 2024; Xue et al., 2019). Water injection development has been widely used in oilfield development as an essential means of maintaining formation pressure and improving oil and gas recovery (Chen, 2021; Yu et al., 2024). However, reservoirs' physical properties are gradually altered by long-term water injection development, especially in oilfields where water injection development and multilayer combined recovery methods are used. As water injection continues, reservoir properties change significantly, leading to increased formation inhomogeneity and decreased recovery efficiency (Hu et al., 2017; Song, 2020).

A key effect of long-term water injection is the further intensification of physical differences between high-permeability and low-permeability formations. Over time, this difference becomes more pronounced, making the problem of nonhomogeneity in a reservoir more prominent (Rajbongshi et al., 2024). The injected water and side water flow forward unevenly in the formation along the high-permeability layer and rarely enter the middle- and low-permeability layers, resulting in the phenomenon of finger-in (Gomaa et al., 2024), which causes a rapid rise in well water cuts and decreases oil and gas recovery rates (Li et al., 2020; Tang, 2007). High water cuts have become a key challenge that seriously restricts efficient oilfield development. Most oilfields are

* Corresponding author.
E-mail address: lizhzh9@cnooc.com.cn (Z. Li).
Peer review under the responsibility of Editorial Office of Petroleum Research.

https://doi.org/10.1016/j.ptlrs.2025.11.008
2096-2495/© 2025 Chinese Petroleum Society. Publishing services by Elsevier B.V. on behalf of KeAi Communications Co. Ltd. This is an open access article under the CC BY-NC-ND license (http://creativecommons.org/licenses/by-nc-nd/4.0/).

now in a high water cut period, and according to statistics, the comprehensive water cut rate of the Bohai oilfields has reached 87.74%, and the water cut rate of some oilfields even exceeds 95%. The Bohai Oilfields are China's largest offshore crude oil production base, located in the Bohai Bay. Operated by China National Offshore Oil Corporation (CNOOC), it encompasses over 50 fields and 200 facilities, producing about 720,000 barrels of crude daily in 2024. Recent developments include the start of production at the Kenli 10-2 oilfield and the discovery of the Qinhuangdao 27-3 oilfield, which bolster China's energy security and its economic development. Among these, high water cut wells represent 26.7% of all low-production and low-efficiency wells (Liu et al., 2024; Zhou et al., 2022).

Current offshore oilfield water-control practices predominantly employ completion and formation-based methodologies. Among the established completion-oriented technologies, inflow control devices, autonomous inflow control devices, and continuous packer systems have been widely implemented (Gao et al., 2023; Zhang et al., 2021a, 2021b). Although these mechanical isolation methods effectively restrict water influx by sealing off water-bearing intervals, their broader applicability is constrained by inherent complexities, substantial operational costs, and a critical reliance on accurately determining the exact locations of water breakthroughs within a wellbore. Consequently, such limitations present considerable obstacles to maintaining stable production and achieving optimal reservoir exploitation, particularly in mature oilfields and thin, interbedded reservoirs.

Early water breakthrough and high water percentages in oil wells have become the main factors affecting well production capacity, reducing development efficiency and accelerating production decline. To solve the negative impacts of high water cuts and improve the recovery efficiency of water drives, chemical water-control technology is widely used in oilfield development. Currently, the most commonly used chemical water-control materials mainly include gels and freeze-gel type plugging agents. These agents rely on physical blocking to form a barrier in highly permeable layers, thereby improving the reach of water drives and slowing down the rapid flow of water. However, these plugging agents have limitations, such as poor selectivity, high injection pressure, and susceptibility to reservoir damage (Liang et al., 2023; Zhao et al., 2016). Also, Distinguishing between oil-bearing formations and water passages is typically challenging, which may result in accidently sealing productive oil formations, thereby reducing well output and compromising overall recovery effectiveness. This type of plugging agent may also lead to irreversible blocking, making subsequent development more difficult and even causing long-term damage to reservoir permeability.

In addition to gels and freeze-gels, foams, thick oils, and hydrolyzed polyacrylamide based plugging agents are widely used to enhance the selective blocking of water. These materials can, to a certain extent, regulate permeability and enhance flow resistance to the aqueous phase. However, they generally exhibit defects, such as short effective periods, insufficient high-temperature resistance, limited blocking efficiency, and even serious well-plugging problems during plugging agent injection, which limit their practical application effects in complex reservoir environments (Deng et al., 2021; Fang et al., 2012; Zhang et al., 2022). Therefore, there is an urgent need to develop and apply a new type of water-control material that can more widely, efficiently, stably, and economically achieve reasonable water control in various formations, improving the current issues of poor reservoir homogeneity and low recovery efficiency.

This study focused on the development characteristics of offshore oilfields. An oil-soluble polymer was synthesized by emulsion polymerization, and a high-selectivity water control system was developed using a water-dispersible method. The water-control performance and mechanism of action were tested and analyzed using various methods, with a particular emphasis on addressing the oil–water selectivity issue of water-control materials for oil wells. By combining the material's nanoscale particle size with its excellent water-blocking and oil-dissolving selective water-control performance, the material achieved good injectability and selective water-control effects in reservoirs with varying permeability and completion screens of different sizes.

2. Materials and methods

2.1. Materials and instruments

2.1.1. Materials

The following chemicals were used for this experimental study: Octadecyl methacrylate (Shanghai Aladdin, analytical reagent); butyl methacrylate (Hengfeng Petrochemical Co, industrial grade), butyl methacrylate (Hengfeng Petrochemical, industrial grade); Tween-80 (Tianjin Damo, analytical reagent), oleic acid (Tianjin Damo, analytical reagent), Span-80 (Tianjin Kemiou Chemical Reagent Co., Ltd., analytical reagent), potassium persulfate (KPS, Shanghai Macklin, analytical reagent), 2,2′-Azobis(isobutyronitrile) dihydrochloride (V50, Shanghai Macklin, analytical reagent), and a nonionic surfactant YCA-1 (self-developed, industrial grade).

2.1.2. Instruments

The following instruments were employed in this experimental study: PURA II Constant Temperature Water Bath (JULABO Technology (Beijing) Co., Ltd.); PL403-IC Electronic Balance (Mettler Toledo Instruments (Shanghai) Co., Ltd.); DF-101S Heating Magnetic Stirrer (Shanghai Licheng Bangxi Instrument Technology Co., Ltd.); Nitrogen Bottle (Liquefied Air (Tianjin) Co., Ltd.); JRJ300-SH High-Speed Shear Emulsifier (Shanghai Huxi); BT-9300H Laser Particle Size Analyzer (Dandong Baiter); Core Holder and Sand-Filling Tube (Sichuan Gaoping Precision); Waters 515 HPLC Pump (Waters Corporation, USA); Hitachi-7700 Transmission Electron Microscope (Hitachi, Japan); PHENOM-WORLD Pure Scanning Electron Microscope (Phenom-World, Netherlands); Visual Plate Displacement Device (Shandong Shida Ke Instrument); Low-Field Nuclear Magnetic Resonance Core Imaging System (Suzhou Tainuo); Binder Oven (Binder GmbH, Germany); Nicolet IS10 Infrared Spectrometer, (Thermo Fisher Scientific, USA).

2.2. Experiments

2.2.1. Preparation of a high-selectivity water control system

Octadecyl methacrylate and butyl methacrylate were used as basic materials. The oil-soluble polymer was synthesized through emulsion polymerization. The product was characterized to confirm the synthesis of the target polymer. The polymer was then emulsified and dispersed to prepare a high-selectivity water control system. Specifically, a certain amount of the oil-soluble polymer was dissolved in white oil, and a certain mass of oleic acid was added to form the oil phase. The mixture was stirred thoroughly and set aside. Next, a certain mass of nonionic surfactant YCA-1 was added to tap water to form the water phase, and this mixture was stirred thoroughly. The oil phase was heated to 90 °C and stirred at 15,000 rpm. After 0.5 h–1 h, the aqueous solution of YCA-1 was slowly added dropwise, and stirring was continued for 2–3 h to obtain a high-selectivity water control system. The schematic diagram of the highly selective water control system preparation is shown in Fig 1.

2.2.2. Fourier transform infrared spectroscopy characterization

Specific characteristic stretching vibration bands within the obtained spectra were analyzed to identify the functional groups and chemical bonds present in the samples (Xie et al., 2022). Analytical-grade potassium bromide (KBr) was oven-dried at 120 °C for 4–6 h before analysis. Subsequently, each dried sample was homogenized with KBr powder at a mass ratio of 1:100 through uniform and unidirectional grinding for approximately 10–15 min, yielding a fine and homogeneous mixture. This mixture was compressed under optimized pressure into translucent pellets and handled exclusively using tweezers to avoid contamination. Before sample analysis, background spectra were obtained from pure KBr pellets. The sample spectra were acquired by scanning within the spectral range of 400 cm^{-1}-4000 cm^{-1}.

2.2.3. Laser diffraction analysis

The high-selectivity water control system operates via a carefully engineered mechanism: upon demulsification within the reservoir, oil-soluble particulates are released and subsequently assembled into bridging plugs within the reservoir pore throats, thereby enabling selective water blockage. Given that the effectiveness of bridging critically depends on particle size distribution, accurate determination of the median particle size of the emulsified system is essential (Sun, 2020). With reference to GB/T 19077-2016 "Particle Size Analysis: Laser Diffraction Methods," the particle size of the emulsion droplets of the high-selectivity water control system was tested using a BT-9300H laser particle size analyzer (SAC, 2016). At room temperature, 0.1 mL of the high-selectivity water control system, after being well dispersed, was placed in the sample pool. The sample was introduced with pure water to eliminate air bubbles, and the particle size distribution was measured. The test was repeated twice, and the final results were obtained.

2.2.4. Reservoir stability test of a high-selectivity water control system

The emulsion stability was tested according to GB/T 11543-2008 "Surface Active Agents: The Identification of Emulsion for Moderate to High Viscosity and the Evaluation Method of Emulsifying Capability" (SAC, 2008) and GB/T 11175-2021 "Testing Methods for Synthetic Resin Emulsions" (SAC, 2021). The emulsion system was diluted to 10% with seawater and subjected to centrifugal testing at 60 ± 2 °C, 70 ± 2 °C, and 80 ± 2 °C under a rotation speed of 2000 rpm for 30 min. After centrifugation, the samples were observed to check for phase separation or oil–water separation at different time intervals. Also, the morphology of the emulsion before and after demulsification was characterized using a Hitachi-7700 transmission electron microscope (TEM) at a voltage of 100 kV.

2.2.5. Selectivity and erosion resistance testing

The selective water-control performance and erosion resistance of a highly selective water-control agent in a reservoir were tested using a core displacement test. The core used in this test is an artificial core with a permeability of 1500 mD. The experimental method was carried out according to SY/T 5336-2006 "Practices for Core Analysis," and the device is shown in Fig. 2 (PSCOGD, 2006). The experiment was divided into two parts: #1 core was used for the water-phase plugging test. Based on core pretreatment, the core displacement experiment was carried out according to the process of saturated water-plugging agent injection-high temperature aging-reverse water flooding. The oil-phase displacement experiment was carried out on the #2 core. Based on core pretreatment, the core displacement experiment was carried out according to the process of saturated water-saturated oil-plugging agent injection-high temperature aging-reverse oil displacement.

According to the measured value of the injection pressure of the displacement experiment, combined with the Darcy formula, the initial state permeability (oil and water two phases) and the permeability after plugging (oil and water two phases) of the physical model core were respectively calculated to calculate the selective plugging ability of the plugging agent under different permeability conditions. The erosion resistance test was based on the reverse displacement of #1 core water, and the simulated formation water was continuously injected at a flow rate of 1 mL/min for more than 50 PV, and the change of inlet pressure was observed to evaluate the erosion resistance of the system (Li et al., 2022).

2.2.6. Visual plate displacement experiment

The selective water-control performance of the system in heterogeneous reservoirs was observed by a plate displacement experiment. The experiment was carried out using the plate sand-filling method. The middle of the plate was a high-permeability reservoir, and the surrounding area was a low-permeability reservoir. First, the saturated oil (red) in the plate was displaced at a flow rate of 1 mL/min, and then the saturated water (blue) at the same flow rate was used to observe the distribution of the water and oil phases. Under the same conditions, the experiment was carried out again, and the injection sequence was the oil phase, water control system, and water phase. The distribution of the oil–water two-phase was observed.

2.2.7. Low-field nuclear magnetic resonance (NMR) evaluation of core displacement and fluid distribution

The experiment was conducted using a natural core with a permeability of 1500 mD. Initially, the core was saturated with simulated formation water, and the water-phase distribution in the core was evaluated using a low-field NMR scanner (e.g., the Hitachi-7700 model). The scanning parameters were set as follows: echo time (ET) of 2 ms, repetition time (RT) of 2000 ms, and scan resolution of 1024 points.

The core was then injected into the water control system for forward displacement, and the distribution of the water control agent within the core was analyzed using the same scanning parameters. Subsequently, the core was immersed in simulated formation water and aged at 80 °C for 12 h. After aging, heavy water was injected for reverse flooding, and the core was scanned using the same conditions to evaluate the distribution of the water phase and the water control agent in the core. Finally, simulated oil was injected into the core for reverse flooding. After the flow rate stabilized, the core was scanned again to observe the distribution of the oil phase and the water control agent. The T_2 spectra were analyzed to evaluate the interactions and distribution of oil, water, and the water control agent.

3. Results and discussion

3.1. FT-IR characterization of the oil-soluble polymer

Fourier transform infrared (FT-IR) spectra of the samples were obtained using a Bruker TENSOR II FT-IR spectrometer and the attenuated total reflectance method (Fig. 3). The absorption peaks at 2920 cm^{-1} and 2851 cm^{-1} corresponded to the symmetric and asymmetric stretching vibrations of the carbon-hydrogen bonds in the methyl (-CH_3) and methylene (–CH_2–) groups, respectively. The absorption peak observed at 1633 cm^{-1} corresponded to the bending vibration mode (H–O–H) of molecular water, while the broad peak centered at 3431 cm^{-1} was assigned to the asymmetric

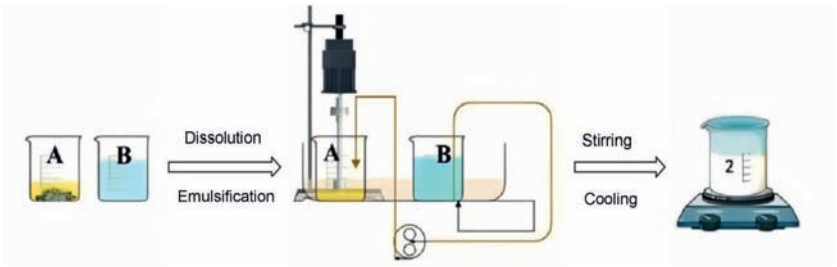


Fig. 1. Schematic of the preparation of the high-selectivity water control system.

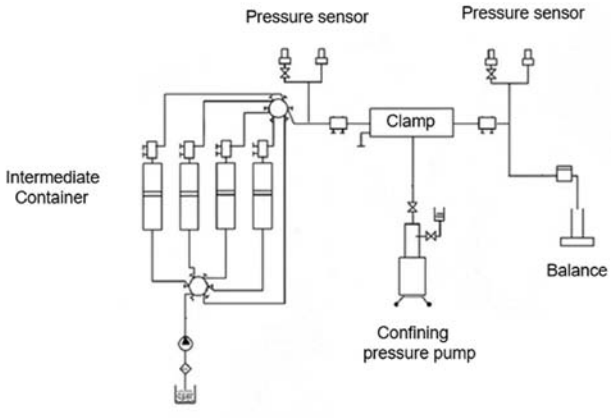


Fig. 2. Core displacement device.

stretching vibration (O–H) of hydroxyl groups associated with absorbed water molecules.

A characteristic absorption peak for the C═O stretching vibration of the ester group appeared at 1732 cm^{-1}, confirming the successful polymerization of octadecyl methacrylate. The peaks at 1470 cm^{-1} and 1150 cm^{-1} were attributed to the symmetric stretching vibrations of the carboxyl carbon-oxygen single bond (C–O), while the peak at 722 cm^{-1} corresponded to the out-of-plane bending vibration of C–C. Additionally, no absorption peak was observed in the range of 1620 cm^{-1} to 1680 cm^{-1}, which is a typical vibration absorption peak of the C═C bond, indicating that the product does not contain carbon–carbon double bonds and that there are no residual monomers in the system. Based on these results, it can be concluded that the polymer is the target product (Gao, 2005).

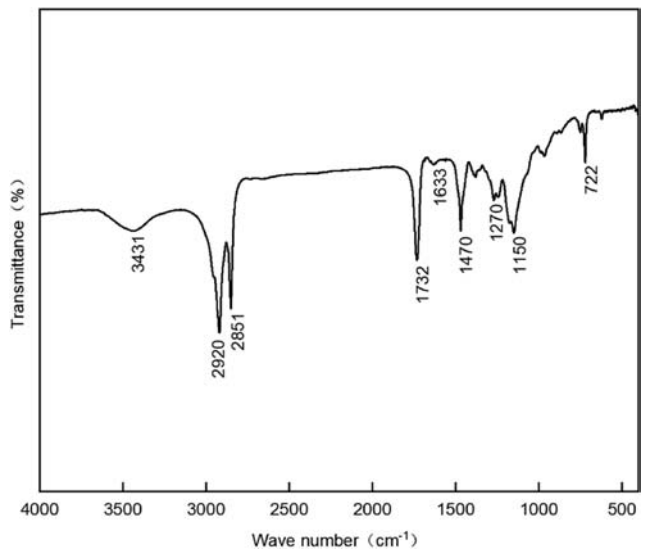


Fig. 3. Fourier transform infrared of the oil-soluble polymer.

3.2. Median particle size testing

The mechanism of a highly selective water-control system is that the system releases oil-soluble particles after demulsification in a reservoir, and the particles form a bridge in the pore throat to exert selective water-control performance. The bridge theory is closely related to particle size, so it is necessary to test the median particle size of an emulsion system. To improve the reservoir injectivity of the material, the oil-soluble polymer was prepared into a water-dispersible emulsion system to ensure its ability to enter the deep reservoir during the on-site construction process. Therefore, it was extremely necessary to test the particle size distribution of the emulsion. The particle size distribution was measured using a laser particle size analyzer. The experimental results are shown in Fig. 4. It can be seen from the experimental results that the median droplet size D50 in the system was 0.431 μm, D90 was 0.530 μm, showing a normal distribution, and the distribution range was 0.431 μm–0.862 μm. It can be seen that the droplet size in the system was small and evenly dispersed, which met the requirements of injection and bridging in the pore throat of the reservoir during field construction.

The experimental results indicate that the emulsion system exhibits a normal droplet size distribution characterized by a median diameter (D_{50}) of 0.431 μm and a D_{90} value of 0.530 μm, with an overall particle size range of 0.431 μm–0.862 μm. This distribution signifies favorable attributes, including uniformly dispersed droplets of a sufficiently small size. Petrophysical analyses of the target reservoir block indicate advantageous reservoir characteristics, with gas permeability (K) ranging between 1193.1 mD and 1436 mD, and porosity (φ) measured at 29.8%.

Applying the established empirical relationship between permeability and pore-throat diameter $D = 2\tau\sqrt{8k/\varphi}$ (with tortuosity (τ) assumed to be between 1.2 and 1.5) (Liu, 2018), the calculated pore-throat diameters ranged from 1.938 μm to 2.423 μm. According to Abrams' temporary plugging theory (Cui, 2022), effective bridging and sealing of reservoir pore throats by solid particles requires compliance with the bridging rule; particle diameters should range from approximately one-third to one-seventh of the pore-throat diameter to facilitate entry and ensure stable bridging. Thus, the measured droplet size distribution satisfied both the injectivity constraints for practical field application and the theoretical criteria necessary for effective bridging within the reservoir pore network.

3.3. Reservoir stability of high-selectivity water control systems

According to the water control principle of the system and the requirements of on-site construction, the emulsion system should have the following properties: It is stable in the conventional storage state, and after entering the formation, demulsification occurs under the action of a certain temperature and salinity water to release the oil-soluble particles. Therefore, it was necessary to test the reservoir stability of the system according to the construction time and to observe the state changes of the system particles before and after demulsification. The test temperature was the target reservoir temperature of the Bohai Oilfield, and simulated formation water with 30,000 mg/L salinity was used. The results are shown in Table 1 and Fig. 5.

According to the experimental results, the prepared oil-soluble particle emulsion system can be stable for at least 8 h under reservoir conditions. As the temperature increased, the stability of the emulsion gradually decreased. When the temperature reached 80 °C, the demulsification time was about 10 h, which met the injection time requirements during the construction process (>2 h). The TEM images of the emulsion particles before and after demulsification are shown in Fig. 5(a), revealing that the emulsion droplets have a diameter of about 700 nm, a wall thickness of about 33 nm, and a regular spherical shape with a smooth surface. Fig. 5(b) reveals that the oil-soluble material has an obvious network structure after demulsification (as shown in the red circle). Through the above experiments, it was proven that the action principle of the emulsion is completely consistent with the principle of water control.

3.4. Water control performance evaluation

3.4.1. Determination of driving conditions

Core displacement experiments were conducted using native reservoir core plugs exhibiting a permeability of 1436 mD, employing simulated formation water as the displacement fluid. The displacement flow rate was selected based on a velocity sensitivity evaluation of the target reservoir. According to the 2021 velocity sensitivity testing report from the Bohai Experimental Center (CNOOC Bohai Oilfield) (Fig. 6), permeability damage exceeded the threshold of 20% when flow rates reached or surpassed 1.5 mL/min, specifically registering 20.21% at this flow rate. Therefore, to mitigate potential formation damage, a displacement flow rate of 1.0 mL/min was selected for subsequent experiments (PSCOGD, 2010).

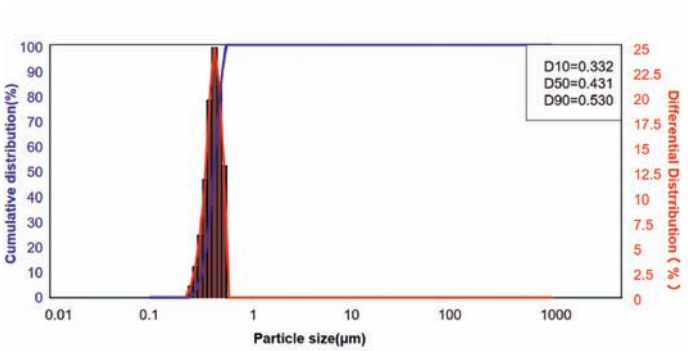
Following the determination of the optimal displacement flow rate (1.0 mL/min), coreflood experiments were conducted by injecting the water control system at varying concentrations. Stable injection pressures were continuously monitored and recorded at each concentration tested. Operational design parameters—including pump rate, drainage radius, net pay thickness, and wellbore friction (Table 2)—along with the target reservoir's fracture pressure (42.94 MPa, as documented in the completion report) were employed to calculate a maximum allowable pump pressure of 34.352 MPa, applying a fracture pressure safety factor of 0.8 (SAC, 2018). Based on these considerations, system concentrations $\leq$14% were determined to be operationally feasible. To achieve an optimal balance between operational performance and economic viability, a concentration of 10% was preliminarily selected for subsequent water-control performance evaluations.

3.4.2. Core selective water control performance

A core with a permeability of 1500 mD was selected to carry out a selective plugging test. The core size was $\varphi 25 \times 100$ mm, and the concentration of the plugging agent was 10%. The #1 core after drying was taken, and the fluid (simulated formation water or formation water) was injected forward at a flow rate of 1 mL/min from one end of the core. When the injection pressure was stable, the injection was stopped, and the original water-phase permeability K_1 was calculated. Then, the system was injected into the core at a flow rate of 1 mL/min, and the displacement was stopped after 2–3 PV when the injection pressure was stable.

After the system injection, the core was aged for 24–48 h at reservoir temperature. The aged core was taken, and the simulated formation water was displaced in reverse. When the pressure was stable, the injection was stopped, and the water-phase permeability K_2 after plugging was calculated. After the water-phase displacement test, the simulated oil was used to test another #2 core with the same permeability, and the original permeability of the oil phase and the permeability of the oil phase after plugging were tested and calculated. The selective plugging property of the system is evaluated by the change in water phase and oil-phase permeability before and after injection into the core (Chen et al., 2024). The results are shown in Fig. 7 and Table 2.

As can be seen in Fig. 6 and Table 2, when the water was displaced in the opposite direction after plugging, the pressure tended to be stable after the displacement volume was about 10 PV, which was 0.033 MPa, much higher than the original water-phase pressure of 0.006 MPa. After plugging, the stable pressure was 0.021 MPa when the oil-phase displacement was about 3.7 PV, and the pressure rise was smaller than the original oil-phase pressure of 0.019 MPa. According to the test results, the water-phase permeability of the core after injection of the system decreased



Particle Size Distribution Summary Table

Size/μm	Content/%
0.000-0.020	0.00
0.020-0.050	0.00
0.050-0.100	0.00
0.100-0.200	0.00
0.200-0.500	81.37
0.500-1.000	18.63
1.000-2.000	0.00
2.000-5.000	0.00
5.000-10.00	0.00
10.00-20.00	0.00

Fig. 4. Particle size distribution of lotion.

Table 1
Reservoir stability test.

Temp.	8 h	10 h	12 h	16 h	20 h	24 h
60 °C	Homogeneous and stable	Homogeneous and stable	Start stratification	Emulsion breaking	Emulsion breaking	Emulsion breaking
70 °C	Homogeneous and stable	Homogeneous and stable	Start stratification	Emulsion breaking	Emulsion breaking	Emulsion breaking
80 °C	Homogeneous and stable	Start stratification	Emulsion breaking	Emulsion breaking	Emulsion breaking	Emulsion breaking

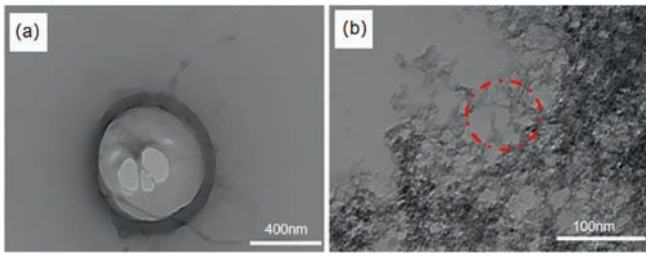


Fig. 5. TEM of the lotion before and after demulsification: (a) emulsion diluted 100 times; (b) oil-soluble materials in emulsion after demulsification.

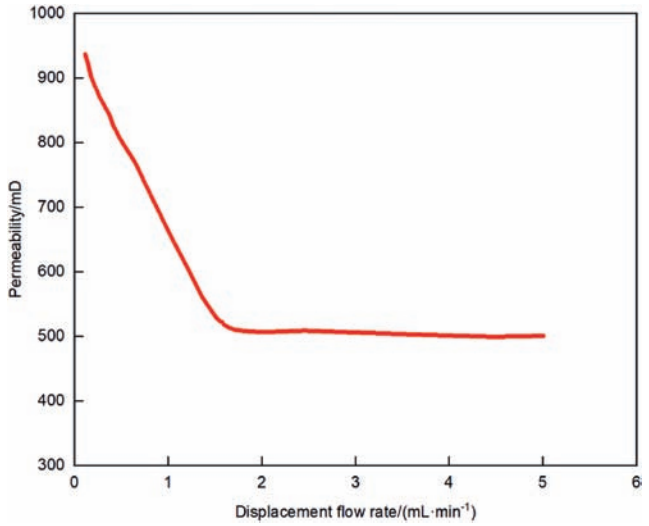


Fig. 6. Velocity sensitivity test curve.

by 82.42% compared with that before plugging, while the oil-phase permeability decreased slightly, with a decrease rate of 5.02%. Therefore, the system had good selective plugging.

3.4.3. *Resistance to flushing*

The erosion resistance of a highly selective water control system depends on the adsorption performance of the material and on its bridging and softening adhesion in the pore throat. During the injection process of the system, emulsion dispersion ensures that the particles are injected and distributed in the reservoir in a state of uniform dispersion and uniform particle size. After the system demulsifies and releases the particles, the particles are bridged under reservoir conditions. Therefore, research on the erosion resistance of water control materials can be carried out through the particle size change state of the plugging agent and a displacement

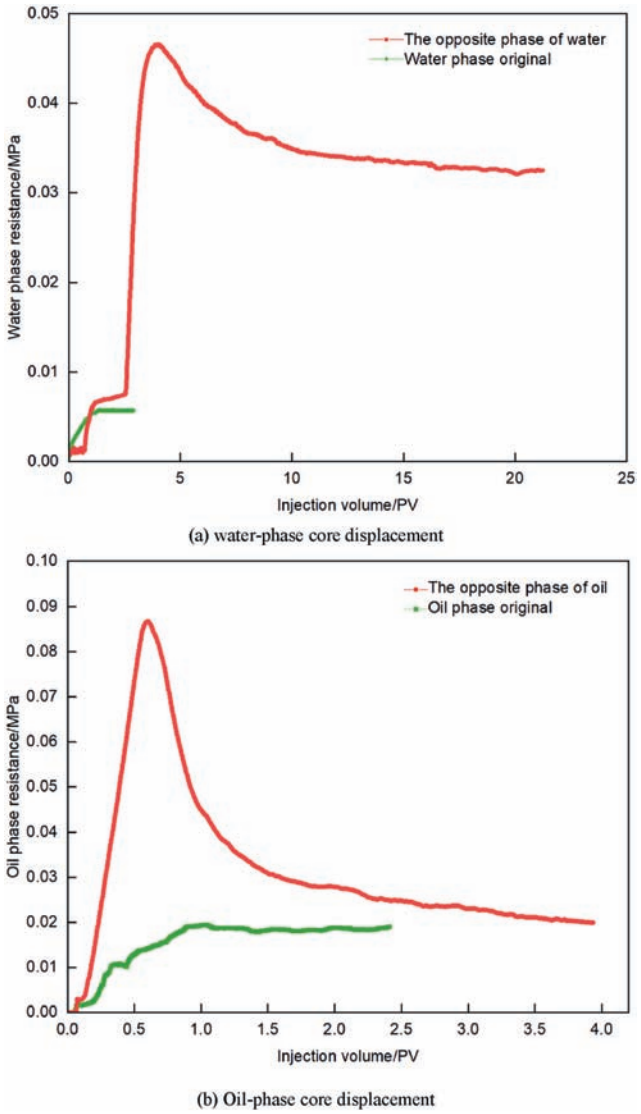


Fig. 7. Core selective water control performance.

evaluation experiment. To maintain the long-term effectiveness of the water control system in the reservoir, it is necessary to have good erosion resistance in the oil well production process to prolong the water control time of the water control system. Therefore, the erosion resistance of the system in the core was evaluated indoors. The experimental results are shown in Fig. 8.

Table 2
System selectivity record table.

Core	Fluid Type	Primitive Penetrance (mD)	Reverse Permeability (mD)	Permeability Decline Rate (%)
#1	Simulation formation water	601.43	105.71	82.42%
#2	Model oil	545.30	517.90	5.02%

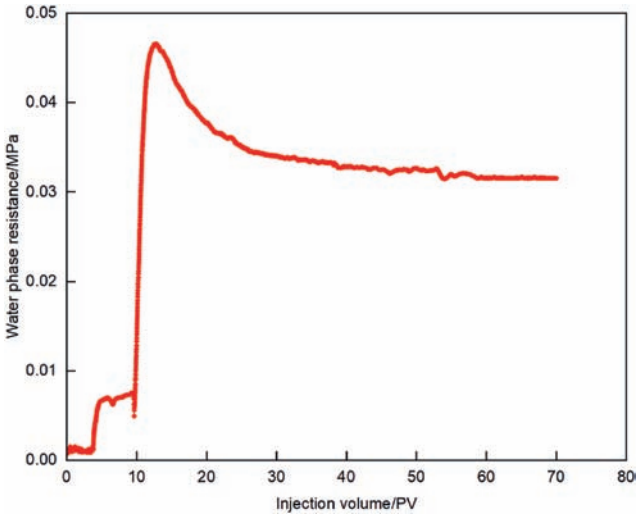


Fig. 8. Evaluation of erosion resistance of the system.

It can be seen from the change law of the water reverse displacement curve that although the displacement pressure fluctuated during the reverse displacement process, it was generally stable and remained at 0.032 MPa without a pressure drop, and there was no sudden decrease in pressure. However, in the process of reverse displacement, the whole flooding liquid was clear and uniform, and no oil-soluble polymer was washed out, which revealed that the water control system has a certain erosion resistance.

3.5. Visual evaluation of water control performance and mechanism analysis

3.5.1. Tablet model displacement test

According to the experimental results (Fig. 9), in the plate that was not injected with the water control material after saturating with oil (brown), water flooding was performed, and the water phase (blue) flowed through the high-permeability channels. In contrast, after saturating another plate with oil (brown) and injecting the material, followed by water flooding, it can be observed that after the high-permeability channels were blocked, the water phase (blue) was distributed along the low-permeability channels. This demonstrates that the material exhibits selective water-control performance.

3.5.2. The NMR of core displacement and fluid distribution

To validate the mechanism and effectiveness of the oil-soluble water control material in the core, low-field NMR scanning was performed during the injection, water flooding, and oil flooding

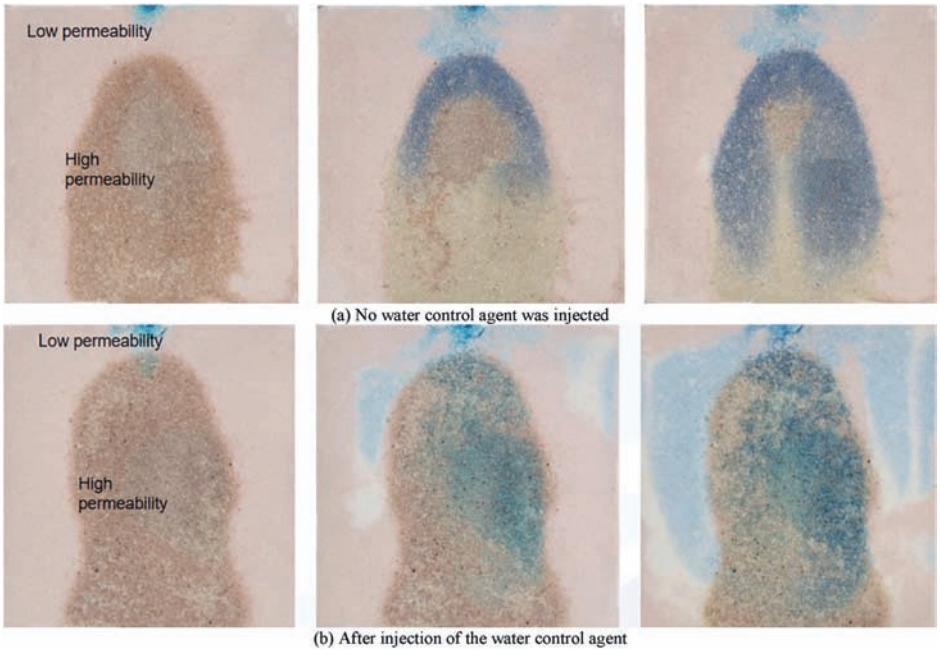


Fig. 9. Tablet model displacement test.

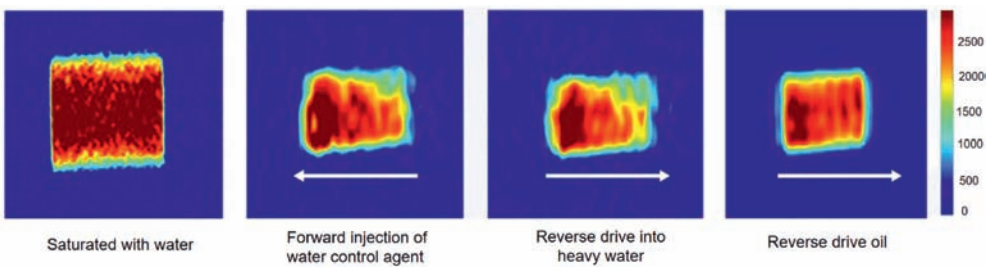


Fig. 10. Low-field nuclear magnetic displacement test (the transition from blue to red indicates an increase in oil signals).

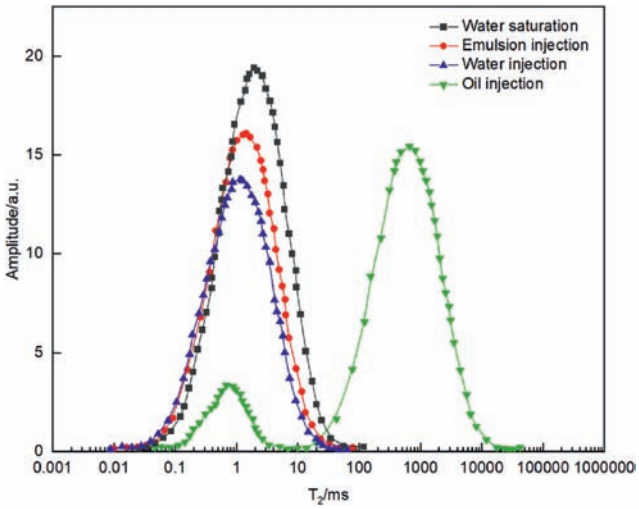


Fig. 11. Low-field nuclear magnetic displacement T2 spectrum.

processes. According to the experimental results (Fig. 10), after saturating the core with oil, the water-phase signal was clear and uniformly distributed (red). After injecting the system, it was observed that it exhibited good injectability in the core. After reverse water flooding, the water phase bypassed the material, and the water control material did not undergo dilution or dissolution, demonstrating selective water control. After the oil-phase injection, the oil phase was evenly distributed in the core (red), and it merged seamlessly with the oil-soluble material, showing excellent oil-solubility performance.

According to the low-field NMR T_2 spectrum shown in Fig. 11, the performance of the core under different fluid injection conditions provides an in-depth analysis of the water plugging and non-oil-plugging characteristics of oil-soluble nanomaterials. In the experiment, the core was first saturated by water, showing that the peak value of saturated water in the T_2 spectrum was the highest, indicating that the water completely filled the pores in the core. When the nanowater-control material emulsion was injected, the peak value in the T_2 spectrum was significantly reduced, indicating that the plugging effect of oil-soluble nanomaterials on pores limited the flow and distribution of water in the core.

After water flooding, the peak change of the T_2 spectrum was basically unchanged, indicating that the oil-soluble nanomaterials will not be washed away under the displacement of water, which further verified that it has good water insolubility. After the final injection of oil, the peak value in the T_2 spectrum increased again, indicating that the oil-soluble nanomaterials were washed by the oil-phase fluid and removed from the pores so that the pore structure was restored. This further reflects the effectiveness of the

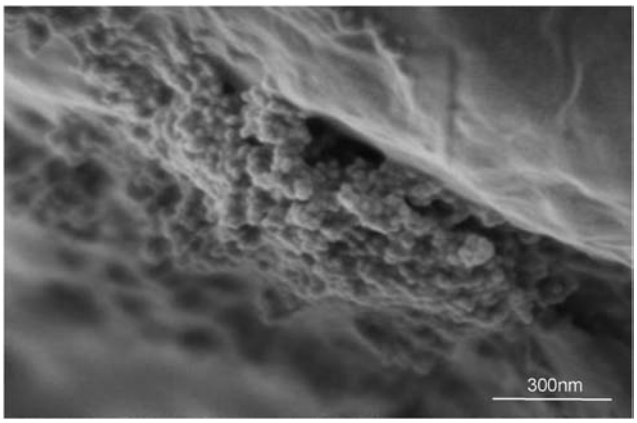


Fig. 13. Microscopic morphology of plugging agent particles in the throat.

nanomaterials in the water-plugging process and the reversible characteristics in the oil flooding process; that is, they can play a plugging role in the water flooding process, and do not hinder the flooding process of oil.

3.5.3. Analysis of the System's water control mechanism

The mechanism of the high-selectivity water control agent primarily involved the following process: after the emulsion system was pumped into the formation pore throats during field operation, it underwent demulsification under reservoir temperature and mineralization of the formation water. Upon demulsification, oil-soluble polymer particles were released. These oil-soluble polymer particles were elastic spherical solids under high temperatures and accumulated to form bridges in the pore-throat channels, achieving the water-blocking effect. The plugging mode followed Abram's temporary plugging theory, where particles with a size range of 1/7–1/3 of the pore-throat diameter could enter the pore throat and block it through bridging, which was the purpose of testing the median particle size of the system (Cui, 2022).

Under the bridging action, combined with the oil-soluble polymer's characteristics of being oil-soluble and water-insoluble, the particles blocked the pore throats when the water phase passed through the formation fluid. When the oil phase passed through, the particles slowly dissolved due to the oil phase and reservoir temperature, ultimately achieving selective water control (Fig. 12). Furthermore, after the core sample was taken post-injection and observed under a scanning electron microscope (Fig. 13), it was observed that after demulsification, the oil-soluble particles could accumulate in the core pore throats and fracture to form a blockage, further verifying the mechanism of action of the system in the reservoir.

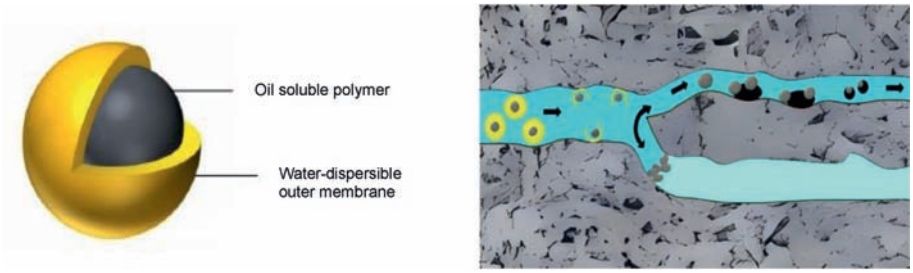


Fig. 12. Schematic diagram of the mechanism of a high-selectivity water control system.

4. Conclusion

In conclusion, we can draw the following conclusions.

(1) An oil-soluble polymer was synthesized using emulsion polymerization with octadecyl methacrylate and butyl methacrylate as comonomers. The polymer was emulsified and dispersed to form a nanoscale, water-dispersible, high-selectivity water control agent. The emulsion showed uniform dispersion with small droplets, having a median droplet size of 0.431 μm and a D90 value of 0.530 μm. The distribution range is 0.431 μm–0.862 μm, making it suitable for field applications.
(2) Under reservoir conditions, the system remained stable for at least 8 h. As the temperature increased, emulsion stability gradually decreased. When the temperature reached 80 °C, the demulsification time was approximately 10 h, which was sufficient to meet the injection time requirements during construction (greater than 2 h).
(3) Selective water-control performance testing showed that water-phase permeability decreased by 82.42% compared to preplugging permeability, while oil-phase permeability decreased by 5.02%. After 70 PV of water-phase flooding, the pressure remained stable without a significant drop, indicating that the system exhibits excellent selective plugging performance and erosion resistance.
(4) Through visualized plate experiments and low-field NMR core scanning displacement tests, the selective water-control performance and mechanism of the system were further validated. Under reservoir conditions, the system released oil-soluble particles, and via the bridging action and the oil-soluble nature of the particles, it effectively achieved selective water control.

CRediT authorship contribution statement

Zhizhen Li: Writing – original draft, Methodology, Investigation, Data curation, Conceptualization. **Weiyu Chen:** Data curation. **Yanhui Su:** Methodology, Investigation, Formal analysis, Data curation. **Xueli Geng:** Investigation, Data curation, Conceptualization. **Bin Shi:** Writing – original draft, Methodology, Investigation, Data curation. **Xiaobin Zheng:** Writing – review & editing, Validation, Supervision. **Qian Zhou:** Investigation. **Gang Xie:** Investigation.

Declaration of competing interest

The authors declare that they have no known competing financial interests or personal relationships that could have influenced the work reported in this paper.

Acknowledgments

This work was financially supported by the Research Project of Engineering Technology Company, CNOOC Energy Technology & Services Limited (No.SSKJ-CG-GJ-2025-04) and the Director's Fund of the National Key Laboratory of Efficient Development of Offshore Oil and Gas (No.KJQZ-2024-2101).

References

Anikin, O.V., Derevyanko, V.K., Bolotov, A.V., Minkhanov, I.F., Varfolomeev, M.A., Konstantinovich, E.A., Kadysheva, V.A., 2025. Gas enhanced oil recovery methods for offshore oilfields: features, implementation, operational status. Petroleum Research 10 (2), 404–415.
Chen, J.M., 2021. Research and Performance Evaluation of oil-soluble Plugging Agent for Clastic Rocks. China University of Petroleum, Beijing.
Chen, L.X., Jia, C.Z., Zhang, R.J., Yue, P., Jiang, X.J., Wang, J.F., Su, Z., Xiao, Y., Lv, Y., 2024. High-pressure capacity expansion and water injection mechanism and indicator curve model for fractured-vuggy carbonate reservoirs. Petroleum 10 (3), 511–519.
Cui, Y.C., 2022. Study on fractal theory of shielding temporary plugging in fractured reservoirs. Nat. Gas. Ind. 22 (2), 45–47.
Deng, B., Jia, Z.W., Liu, W., Liu, X.Q., Gu, J.W., Ye, W.B., Wen, H.B., Qu, Z.Q., 2021. Selective water plugging technology for horizontal well with screen completion. Energies 14 (4), 791–805.
Fang, S.W., Zhang, L.H., Duan, M., Zhang, J., 2012. Preparation of hydrophobically-modified acrylamide copolymers using poly (ethylene imine) as a photo-initiator and its performance evaluation in Bohai oilfield. Polym. Sci. B 54, 79–87.
Gao, H.B., 2005. Organic Chemistry. Higher Education Press, Beijing.
Gao, S.J., Li, H.T., Nie, S., Ai, Y., Luo, H.W., Li, Y., 2023. Design and numerical simulation study of a novel AICD for water control and gas production in gas Wells. ACS Omega 8 (42), 39052–39066.
Gomaa, S., Salem, K.G., El-hoshoudy, A.N., 2024. Enhanced heavy and extra heavy oil recovery. Current status and new trends. Petroleum 10 (3), 399–410.
Hu, Z.W., Xu, C.G., Yang, B., Huang, Z., Su, W., 2017. Genetic mechanism of the granite buried-hill reservoir of the Penglai 9-1 oilfield in Bohai Sea. Petroleum Research 2 (4), 355–365.
Li, N.Y., Zhu, S.J., Li, Y., Zhao, J.R., Long, B., Chen, F., Wang, E.Z., Feng, W.T., Hu, Y.N., Wang, S.B., Jiang, C., 2024. Fracturing-flooding technology for low permeability reservoirs. A review. Petroleum 10 (2), 202–215.
Li, Z.Z., Peng, G.X., Guan, H.P., Meng, P.W., Ma, L., 2022. Preparation and performance evaluation of a polymer fiber ball profile control agent. Speciality Petrochemicals 39 (2), 32–36.
Li, Z.Z., Shi, B., Ma, L., Wang, B., Du, L.Y., Zheng, X.B., 2020. Laboratory study and application of a solution-type selective water shutoff system. Petrochemical Industry Application 39 (1), 53–61.
Liang, D., Zhang, J., Zhou, W.S., Zhao, H., Zhang, Q.C., Wang, L.Q., 2023. Study on low-heat synergistic chemical profile control and flooding technology in Bohai Oilfield. Front. Energy Res. 11.
Liu, Y.X., Ge, L.Z., Ma, K.Q., Chen, X.M., Zhu, Z.Q., Hou, J.R., 2024. Study on surfactant–polymer flooding after polymer flooding in high-permeability heterogeneous offshore oilfields. A case study of Bohai S oilfield. Polymers 16 (14), 2004–2021.
Liu, Z.M., 2018. Research and Application of Polymer Microspheres in Water Control of Horizontal Wells. Southwest Petroleum University, Chengdu.
Professional Standardization Committee of Oil & Gas Development (PSCOGD), 2006. SY/T 5336-2006, Conventional Core Analysis Methods. Professional Standardization Committee of Oil & Gas Development, Beijing.
Professional Standardization Committee of Oil & Gas Development (PSCOGD), 2010. SY/T 5358-2010, Evaluation Method for Flow Test of Reservoir Sensitivity. Professional Standardization Committee of Oil & Gas Development, Beijing.
Rajbongshi, A., Gogoi, S.B.A., 2024. Review on oilfield produced water and its treatment technologies. Petroleum Research 9 (4), 640–656.
Song, M.S., 2020. Reservoir formation conditions and key technologies for exploration and development in Shengtuo oilfield in Bohai Bay Basin. Petroleum Research 5 (4), 289–303.
Standardization Administration of China (SAC), 2008. GB/T 11543-2008, Surface Active Agents - Determination of Stability of Emulsions and Evaluation of Emulsifying Power for Moderate to High Viscosity. Standardization Administration of China, Beijing.
Standardization Administration of China (SAC), 2016. GB/T 19077-2016, Particle Size Distribution - Laser Diffraction Method. Standardization Administration of China, Beijing.
Standardization Administration of China (SAC), 2018. GB/T 36409-2018, Structural Design Method for self-elevating Platforms - Load and Resistance Factor Design Method. Standardization Administration of China, Beijing.
Standardization Administration of China (SAC), 2021. GB/T 11175-2021, Testing Methods for Synthetic Resin Emulsions. Standardization Administration of China, Beijing.
Sun, R.X., 2020. Development and Performance Evaluation of Deformable Particle Temporary Plugging Agent for Tight Reservoirs. China University of Petroleum, Beijing.
Tang, W., 2007. Application of tracer interpretation technology in Leigong oilfield. Journal of Shengli Oilfield Staff University 2007 (1), 49–50.
Xue, Y.A., Deng, Y.H., Wang, D.Y., Yang, H.F., Lv, D.Y., Kang, K., 2019. Hydrocarbon accumulation conditions and key exploration and development technologies for PL 19–3 oilfield. Petroleum Research 4 (1), 29–51.
Xie, G., Luo, Y.J., Wang, C.L., Deng, M.Y., Bai, Y., 2022. Comparative study on the inhibiting mechanism of inhibitor with primary amine groups and quaternary ammonium groups for sodium bentonite. Petroleum 9 (4), 526–533.
Yonguep, E., Kapiamba, K.F., Kabamba, K.J., Chowdhury, M., 2022. Formation, stabilization and chemical demulsification of crude oil-in-water emulsions: a review. Petroleum Research 7 (4), 459–472.
Yu, H., Tuo, Y.H., Lin, T.J., Li, M., Lian, Z.H., 2024. On how water injection may induce fault reactivation and slippage. A numerical method. Petroleum 10 (4), 646–659.
Zhang, G.H., Li, L.C., Chen, R., Wang, P., Zhang, G.W., Sun, J.W., 2021a. Optimization of AICD water control completion technology for horizontal well in bottom water gas reservoir. E3S Web of Conferences 248 (16), 02056.

Zhang, G.H., Wang, P., Chen, R., Li, L.C., Zhang, X.W., 2021b. An optimization method of horizontal well completion control water and sand. IOP Conf. Ser. Earth Environ. Sci. 621.
Zhang, Z.H., Jin, Y., Zhang, J., Tang, E.G., Wei, Z.J., Liang, D., Li, P.H., 2022. Adaptability study of hot water chemical flooding in offshore heavy oilfields. Geofluids 2022 (6), 1–11.
Zhao, T.H., Xing, J.Y., Pu, W.F., Dong, Z.M., Yuan, C.D., Peng, G.F., Jin, F.Y., Xia, J.J., 2016. Synthesis and property evaluation of a novel polyacrylamide-montmorillonite composite for water shutoff and profile control in high salinity reservoirs. Polym. Compos. 39 (2), 368–376.
Zhou, Z.K., Sun, S.S., Wang, R.X., Dang, W.H., Wang, P., 2022. Sensitivity analysis of water control and oil enhancement effects using continuous isolation technology in Bohai oilfield. China Petroleum and Chemical Standard and Quality 42 (22), 184–186.